ARCHIVES OF ELECTRICAL ENGINEERING VOL. 62(3), pp. 439-447 (2013)

DOI 10.2478/aee-2013-0035

Effect of minimum energy control on steel loss in VR stepper motor*

JAKUB BERNAT, JAKUB KOŁOTA, SŁAWOMIR STĘPIEŃ

Chair of Computer Engineering, Poznan University of Technology
Piotrowo 3a, 60-965 Poznań
*e-mail: Jakub.Kolota@put.poznan.p*l

(Received: 26.06.2012, revised: 09.12.2012)

Abstract: This research presents a 3D FE method for the simulation of the variable reluctance stepper motor dynamics. The proposed model is used to obtain the optimal minimum energy control law that minimizes the energy injected by the controller. The method is based on the strong coupling of field – circuit equations and extended to eddy current, motion and nonlinearity problem. The linearization technique for the coupled problem is presented. Also the lamination of the motor core is considered. In the paper the open – loop control problem is analyzed. The proposed model is validated by the comparison with measurements. Next, to demonstrate the effectiveness of the proposed optimal minimum energy control method is applied. In both cases, the examination of the variable reluctance stepper motor dynamics and the steel loss in the core is presented and compared.

Key words: energy consumption, lamination, finite element methods, optimal control

1. Introduction

The application of stepper motors is widespread. From point of view of the energy consumption there are many challenges to numerical modeling and optimization of these devices [5, 11, 16, 17]. The problem is related to decreasing energy delivered to the motor without loss of their dynamics. There are two ways to perform the request: geometry optimization (including material optimization) or optimal control [1, 8, 12, 13].

The improvement of modeling techniques as such 3D FEM have led to the development of stepper motors that offer significant improvements of the power consumption, loss reduction etc. [2-4, 6, 8, 16]. Presented models do not only consider the forward dynamics but also lamination effects [2, 3, 6, 9, 10, 18]. Papers related to the loss estimation give excellent information on where the energy is lost and what is the effect of excitation on the loss in the steel [3].

* This is extended version of a paper which was presented at the 22th *Symposium on Electromagnetic Phenomena in Nonlinear Circuits*, Pula, Croatia, 26.06-29.06 2012.

In this paper a method of modeling of the variable reluctance stepper motor is described. The FE system of equations is coupled with the electric circuit equations in the one global system of equations [5, 17, 18]. The magnetic nonlinearity is considered by introducing Newton-Raphson procedure to linearize the system of nonlinear equations. Also effects of the core loss lamination are considered by the loss estimator when using **A**-V formulation.

The proposed motor model is validated by the comparison with measurements. Moreover, the intention of this paper is to propose and test the minimum energy control [15] to the developed model and finally confirm that suitable control gave less energy expenditure in the laminated core.

2. Modeling technique

The stepper motors always work within electronic controllers, which convert the step frequency and the motion direction signals to switching states of the input windings. Figure 1 shows the configuration of the motor and the inverter circuit and the sequence of the voltage waveforms.

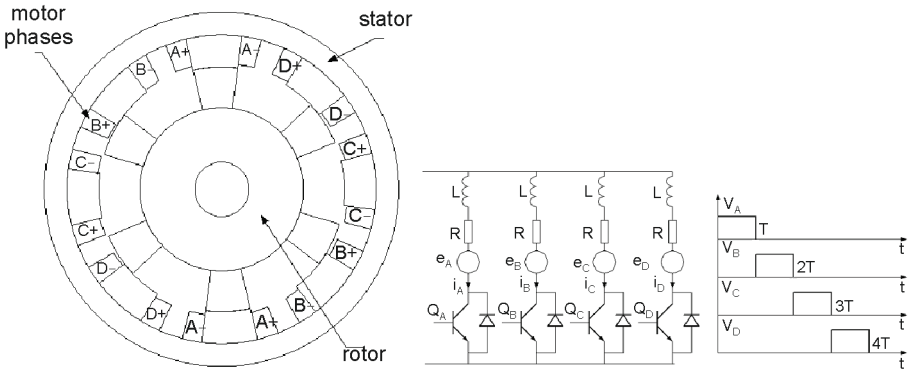

Fig. 1. The motor configuration and the inverter circuit

The governing equations of the electromagnetic field are represented by Maxwell's equations and consider the eddy current problem in the stator and the rotor core:

$$\nabla \times \left(\frac{1}{\mu} \nabla \times \mathbf{A} \right) + \left(\sigma \frac{\partial \mathbf{A}}{\partial t} + \sigma \nabla V - \sigma \mathbf{v} \times (\nabla \times \mathbf{A}) \right) - \mathbf{j} = 0, \tag{1}$$

$$-\nabla \cdot \left(\sigma \frac{\partial \mathbf{A}}{\partial t} + \sigma \nabla V - \sigma \mathbf{v} \times (\nabla \times \mathbf{A}) \right) = 0, \tag{2}$$

where **A** is the magnetic vector potential V is the electric scalar potential, μ is a permeability, σ is the conductivity, $v = \omega \times r$ represents the speed of the rotor and **j** is a current density of the winding.

Due to presence of the ferromagnetic assumption, the nonlinearity of the rotor and the stator materials are considered. The magnetic permeability is a function of the local magnetic field.

The stator phase circuit equation for the described stepper motor is

$$\frac{d}{dt}\oint_{l_s} \mathbf{A}\mathbf{dl} = u_s - Ri_s, \tag{3}$$

where $s = \{1, ..., 4\}$ denotes the phase number, R is the winding resistance of a one phase, i is the phase current and u is the supply voltage.

The rotor displacement is evaluated by solution of the mechanical motion equation:

$$J\frac{d^2\Theta}{dt^2} + b\frac{d\Theta}{dt} = T, \tag{4}$$

where Θ is the rotor displacement, J is the rotor inertia, b is the damping coefficient, T is the difference between the electromagnetic and the load torque.

From the approach (1) – (2) derived is the matrix equation system, where the weighting functions are the same as the shape functions. The solution of the system (1) – (2) is derived by minimizing the corresponding energy functional. The minimization is performed by means of the FE method using 27-node, first order cylindrical elements. The magnetic vector potential may be expressed by

$$\mathbf{A} = \sum_{i=1}^{27} N_i \mathbf{A}_i \ ,$$

where N_i are the element shape functions and the $\mathbf{A}_i$ are the approximations to the vector potentials at the nodes of the elements [15]. Introducing the FE method with the boundary value problem (1) – (2) and coupling to the electric circuit model (3), the following system of equations is obtained in the electromagnetic field:

$$\begin{bmatrix} \mathbf{C}(\mu) + \dfrac{\mathbf{D}}{\Delta t} & \mathbf{E} & \mathbf{K} \\ \dfrac{\mathbf{F}}{\Delta t} - \mathbf{G} & \mathbf{H} & \mathbf{0} \\ \dfrac{\mathbf{L}}{\Delta t} & \mathbf{0} & \mathbf{R} \end{bmatrix} \begin{bmatrix} \mathbf{A}^{t+\Delta t} \\ \mathbf{V}^{t+\Delta t} \\ \mathbf{I}^{t+\Delta t} \end{bmatrix} = \begin{bmatrix} \dfrac{\mathbf{D}}{\Delta t}\mathbf{A}^t \\ \dfrac{\mathbf{F}}{\Delta t}\mathbf{A}^t \\ \mathbf{U}^{t+\Delta t} + \dfrac{\mathbf{L}}{\Delta t}\mathbf{A}^t \end{bmatrix}, \tag{5}$$

where matrix **C** is related to the magnetic field and the induced currents from movement, **D** is related to the induced currents, **E** represents matrix adding a contribution of the electric scalar potential, **K** is related to winding currents, **F** is related to induced currents, **G** related to induced currents from movement, **H** is related to diffusion of the current density, **L** is related to the linkage flux, **R** is related to the winding resistances, **U** is the vector corresponding to the voltage control, **I** is the vector of coil currents.

The presented system of the field Equations (5) is nonsymmetrical and solved at each iteration step by the preconditioned bi-conjugate gradient method.

When considering the magnetic nonlinearity, presented model described by time stepping technique (5) is non-linear. Hence, the system of Equation (5) should be linearized. As mentioned, the Newton-Raphson procedure is applied to linearize the system employing a cubic spline interpolation of an interesting part of the magnetization curve [14]. The linearized form of the global matrix equation system is as follows:

$$\begin{bmatrix} \mathbf{C}(\Delta\mu)+\dfrac{\mathbf{D}}{\Delta t} & \mathbf{E} & \mathbf{K} \\ \dfrac{\mathbf{F}}{\Delta t}-\mathbf{G} & \mathbf{H} & \mathbf{0} \\ \dfrac{\mathbf{L}}{\Delta t} & \mathbf{0} & \mathbf{R} \end{bmatrix} \begin{bmatrix} \Delta\mathbf{A}_{k+1}^{t+\Delta t} \\ \Delta\mathbf{V}_{k+1}^{t+\Delta t} \\ \Delta\mathbf{I}_{k+1}^{t+\Delta t} \end{bmatrix} = -\begin{bmatrix} \mathbf{C}(\Delta\mu)+\dfrac{\mathbf{D}}{\Delta t} & \mathbf{E} & \mathbf{K} \\ \dfrac{\mathbf{F}}{\Delta t}-\mathbf{G} & \mathbf{H} & \mathbf{0} \\ \dfrac{\mathbf{L}}{\Delta t} & \mathbf{0} & \mathbf{R} \end{bmatrix} \begin{bmatrix} \mathbf{A}_{k}^{t+\Delta t} \\ \mathbf{V}_{k}^{t+\Delta t} \\ \mathbf{I}_{k}^{t+\Delta t} \end{bmatrix} + \begin{bmatrix} \dfrac{\mathbf{D}}{\Delta t}\mathbf{A}^{t} \\ \dfrac{\mathbf{F}}{\Delta t}\mathbf{A}^{t} \\ \mathbf{U}^{t+\Delta t}+\dfrac{\mathbf{L}}{\Delta t}\mathbf{A}^{t} \end{bmatrix}, \tag{6}$$

where $\mathbf{C}(\Delta\mu)$ is the matrix related to the permeability change. The dynamic permeability is obtained from the B-H nonlinear curve as $\Delta\mu = \partial B/\partial H$. The potentials and currents update is necessary in the internal computational loop, as long as the permeability correction is performed.

The discrete rotor speed ω and displacement Θ are determined using the backward Euler's approximation for the motion Equation (4)

$$\begin{bmatrix} 1 & -\Delta t \\ 0 & 1+\Delta t\dfrac{b}{J} \end{bmatrix} \begin{bmatrix} \Theta^{t+\Delta t} \\ \omega^{t+\Delta t} \end{bmatrix} = \begin{bmatrix} \Theta^{t} \\ \omega^{t}+\Delta t\dfrac{1}{J}T^{t+\Delta t} \end{bmatrix}. \tag{7}$$

The motion in the electromagnetic field is realized using the fixed grid technique. In this approach the grid of discretisation is independent of the rotor position. The moving body displacement is updating (if necessary) at each iteration step.

The global torque is calculated using the Maxwell stress method. The force is evaluated along with a surface in the airgap around the rotor. The torque component T is obtained from the relationship:

$$T = \oint_{S} \{r \times P\} dS, \tag{8}$$

where **r** is the position vector of the integration contour, **P** denotes the stress component defined around the rotor, **dS** is a surface segment.

3. Minimum energy controller

The aim of the authors is to obtain the optimal control that minimizes the energy delivered to the electric circuit described by the system of four Equations (3). The control problem consists of finding a voltage control vector included in a set of admissible controls D_u, i.e. $\mathbf{U} \in D_u$. The method was applied for a linear model of the stepper motor and based on linear quadratic programming [7, 15]. In this paper the challenge is to employ the control method for the nonlinear, eddy current model.

The voltage control should minimize the objective function

$$J(\mathbf{U}) = \frac{1}{2}\int_0^{\infty} \mathbf{U}^T \mathbf{P}\mathbf{U}\, dt, \tag{9}$$

where $\mathbf{I}$ is the winding currents vector, $\mathbf{U}_T\mathbf{P}\mathbf{U}$ is a function of the power injected by the controller, $\mathbf{P} > 0$ contains the weighting factors. Basing on the linear-quadratic programming for the infinite time horizon, the voltage control function may be determined minimizing (9) i.e. $\min_{\mathbf{U}\in D_u} J(\mathbf{U})$.

When considering the energy in the electric circuit, the source power (9) and right side of (3) may be expressed by the Hamiltonian [7]:

$$H(\mathbf{U},\mathbf{I},\boldsymbol{\Psi}) = \frac{1}{2}\mathbf{U}^T\mathbf{P}\mathbf{U} + \boldsymbol{\Psi}^T(\mathbf{U} - \mathbf{R}\mathbf{I}). \tag{10}$$

From the derivation $\partial H / \partial \mathbf{U} = \mathbf{0}$ it is possible to obtain the optimal control

$$\mathbf{U}^* = -\mathbf{P}^{-1}\boldsymbol{\Psi}. \tag{11}$$

Assuming that the function $\boldsymbol{\Psi} = \boldsymbol{\Gamma}\mathbf{I}$ depends on the current vector $\mathbf{I}$ and $\boldsymbol{\Gamma}$ is a constant feedback gain, the derivation of the $\boldsymbol{\Psi}$ may be calculated from:

$$\frac{d\boldsymbol{\Psi}}{dt} = -\boldsymbol{\Gamma}\mathbf{R}^T\boldsymbol{\Gamma}\mathbf{I}. \tag{12}$$

Using the function $\boldsymbol{\Psi}$ to denote the winding linkage flux vector and employing the optimal control (12), the following relationship is obtained

$$\frac{d}{dt}\left[\oint_{l_1}\mathbf{A}\mathrm{d}\mathbf{l}\oint_{l_2}\mathbf{A}\mathrm{d}\mathbf{l}\oint_{l_3}\mathbf{A}\mathrm{d}\mathbf{l}\oint_{l_4}\mathbf{A}\mathrm{d}\mathbf{l}\right]^T = \mathbf{U}^* - \mathbf{R}\mathbf{I} = -\left(\mathbf{P}^{-1}\boldsymbol{\Gamma} + \mathbf{R}\right)\mathbf{I}. \tag{13}$$

Equating (12) and (13) results in

$$\mathbf{P}^{-1}\boldsymbol{\Gamma} + \mathbf{R} = \boldsymbol{\Gamma}\mathbf{R}^T\boldsymbol{\Gamma}, \tag{14}$$

where $\boldsymbol{\Gamma}$ is an unknown. Using the fact that the resistance matrix is diagonal $\mathbf{R} = \mathbf{R}^T$, then $\boldsymbol{\Gamma}$ may be calculated from the non-linear matrix system of equation:

$$-\boldsymbol{\Gamma}\mathbf{R}\boldsymbol{\Gamma} + \mathbf{P}^{-1}\boldsymbol{\Gamma} + \mathbf{R} = \mathbf{0}. \tag{15}$$

Employing the obtained matrix in (15) to the optimal control definition (11), we may define the voltage control law as the function of the current vector may be defined as $\mathbf{U}^* = -\mathbf{P}^{-1}\boldsymbol{\Gamma}\mathbf{I}$. The obtained control law may be rewritten to the form in which the reference current vector is defined $\mathbf{I}_{ref}$ in the stepper motor windings

$$\mathbf{U}^* = -\mathbf{P}^{-1}\boldsymbol{\Gamma}\left(\mathbf{I} - \mathbf{N}\mathbf{I}_{ref}\right). \tag{16}$$

The matrix gain $\mathbf{N}$ related to the reference current vector I may be determined for the steady state voltage applied on the windings $\mathbf{N} = \boldsymbol{\Gamma}^{-1}\mathbf{P}\mathbf{R} + \mathbf{Y}$, where $\mathbf{Y}$ is the identity matrix.

4. Analysis of the motor model

In the numerical experiment, proposed numerical model has been applied to investigate the step response and current response of the motor. The motor has been examined using the 3D FEM in which eddy currents and nonlinearity are considered. As shown in Figure 2, the mesh includes 0.35 mm Silicon sheets in which the eddy current loss is calculated.

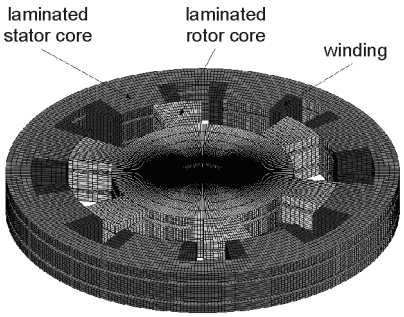

Fig. 2. The mesh of the motor part

To demonstrate the effectiveness of the technique, the step response and the first phase i_1 current course have been examined and compared with measured. The model has been analyzed for the PWM voltage excitation with the amplitude $u = 20$ V. The coil resistance is equal to $R = 12.4\ \Omega$.

The step response has been verified by comparison to the encoder measured response with resolution 400 imp/rev as shown in Figure 3.

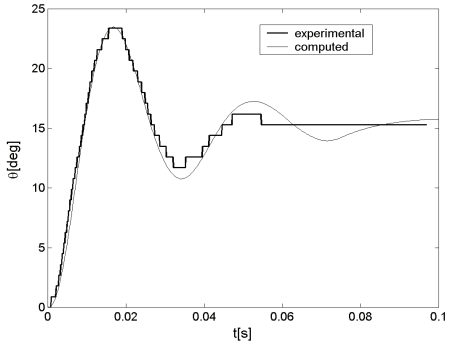

Fig. 3. The step response verification

The phase current has been measured by the Hall effect-based current sensor connected to the first phase. The current amplitude presented on Figure 4 is equal to 1.61 A (1D = 0.35 A). Presented results show good agreement. The figure 5 presents the computed phase current and the results show good agreement

The eddy current losses are calculated based on field results of eddy currents **J** flowing inside rotor and stator sheets [2, 3]:

$$P = \int_{V_r} \frac{|\mathbf{J}|_{rms}^2}{\sigma} dv + \int_{V_s} \frac{|\mathbf{J}|_{rms}^2}{\sigma} dv, \tag{17}$$

where V_r and V_S denote rotor and stator volumes. In the Table 1, the eddy current steel loss computed for the one step operation (100 ms time interval) is presented.

Fig. 4. The measured phase current

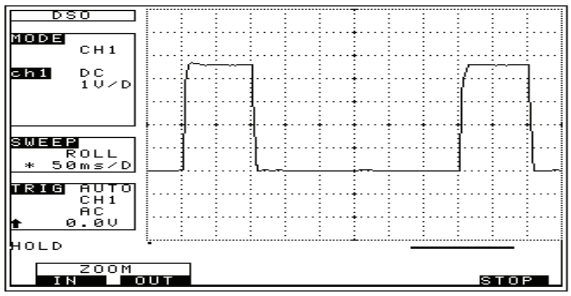

Fig. 5. The computed phase current

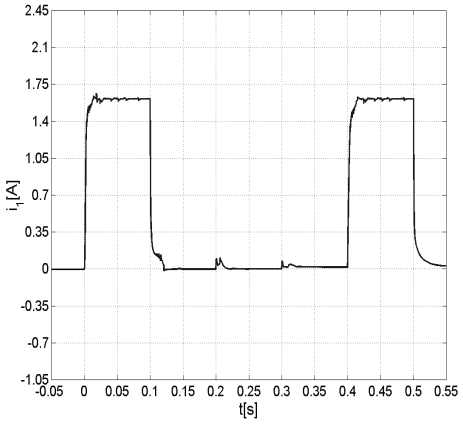

Table 1. Computed eddy current steel loss

Quantity	P [mW]
Steel eddy current steel loss	24.5

5. Analysis of the control problem

To demonstrate the effectiveness of the proposed closed – loop control method, The eddy current losses are computed for the case where the reference current for each phase is i_{ref} = 1.61 A. The **P** matrix defined in (10) is diagonal and defined as the inverse of **R** composed of the winding resistance $\mathbf{P} = diag[1/R\ 1/R\ 1/R\ 1/R]$.

Solving the nonlinear system of Equation (16) using the Newton's iteration, the feedback gain matrix $\mathbf{\Gamma} = -diag[0.618\ 0.618\ 0.618\ 0.618]$ is computed. Also, the input gain matrix is calculated and equals $\mathbf{N} = -diag[0.618\ 0.618\ 0.618\ 0.618]$.

In the control experiment, proposed numerical model has been applied to investigate the step response. The response has been compared to the step response resulted in the last paragraph (computation without optimal control).

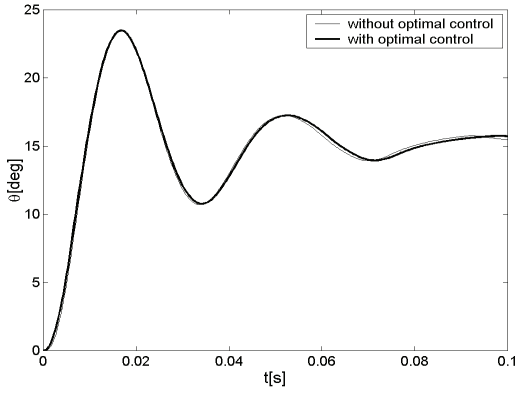

Fig. 6. Comparison of the step responses

The Figure 6, shows the step response comparison between presented control techniques and confirms that optimum control gave the same dynamic performance.

Also, in this case, the value of the eddy current loss is calculated for the one step operation and presented in Table 2.

Table 2. Computed eddy current steel loss considering optimal control

Quantity	P [mW]
Steel eddy current steel loss	21.6

The value of the loss in case of the optimal control is lower, because the control system drives the electric circuit of the motor to the reference current producing less violent rising edge of the voltage and current. In the optimal control mode, the peak loss produced at starting phase of the step is significantly reduced.

6. Conclusions

The paper has examined the nonlinear eddy current field – circuit model of the variable reluctance stepper motor using 3D FEM. Simulation and experiment show good agreement. The proposed model of variable reluctance stepper motor has been used to obtain the optimal minimum energy control law that minimizes the energy injected by the controller.

Using the developed model, the control method has been proposed to reduce the eddy current loss in laminated sheets. The proposed model has been validated by the comparison with measurements. The examination of the stepper motor dynamics and the steel loss in the core is presented and compared. The method confirms that optimum control gave the same dynamic performance with the loss reduction.

References

[1] Bolognani S., Zigliotto M., *Fuzzy logic control of a switched reluctance motor drive.* IEEE Trans. Ind. Appl. 32(5): 1063-1068 (1996).

[2] Cheng Z., Takahashi N., Forghani B. et al., *Effect of Variation of B-H Properties on Loss and Flux Inside Silicon Steel Lamination.* IEEE Trans. Magn. 47(5): 1346-1349 (2011).

[3] Cheng Z., Takahashi N., Forghani B. et al., *Effect of Excitation Patterns on Both Iron Loss and Flux in Solid and Laminated Steel Configurations*. IEEE Trans. Magn. 46(8): 3185-3188 (2010).

[4] Dyck D., Gilbert G., Lowther D.A., *A performance model of an induction motor for transient simulation with a PWM drive.* IEEE Trans. Magn. 46(8): 3093-3100 (2010).

[5] Fu W., Ho S., *Enhanced nonlinear algorithm for the transient analysis of magnetic field and electric circuit coupled problems*. IEEE Trans. Magn. 45(2): 701-706 (2009).

[6] Gyselinck J., Vandevelde L., Melkebeek J. et al., *Calculation of eddy currents and associated losses in electrical steel laminations.* IEEE Trans. Magn. 35(3), (1999).

[7] Haddad W., Chellaboina V., *Nonlinear Dynamical Systems and Control: A Lyapunov-Based Approach.* Princeton University Press (2008).

[8] Krishnan R., *Switched Reluctance Motor Drives. Modeling, Simulation, Analysis, Design, and Applications.*, ser. I. E. Boca Raton, FL: CRC Press (2001).

[9] Lin D., Zhou P., Chen Q. et al., *The Effects of Steel Lamination Core Losses on 3D Transient Magnetic Fields.* IEEE Trans. Magn. 46(8): 3539-3542 (2010).

[10] Lin D., Zhou P., Fu W., Badics Z., Cendes Z., *A dynamic core loss model for soft ferromagnetic and power ferrite materials in transient finite element analysis*. IEEE Trans. Magn. 40(2): 1318-1321 (2004).

[11] Lin D., Zhou P., Stanton S., Cendes Z.J., *An Analytical Circuit Model of Switched Reluctance Motors*. IEEE Trans. Mag. 45(9): 5368-5375 (2009).

[12] Mir S., Islam M., Sebastian T., Husain I., *Fault-tolerant switched reluctance motor drive using adaptive fuzzy logic controller*. IEEE Trans. Power Electron. 19(2): 289-295 (2004).

[13] Paramasivam S., Arumugam R., *Real time hybrid controller implementation for switched reluctance motor drive.* Amer. J. Appl. Sci. 1(4): 284-294 (2004).

[14] Salon S.J., *Finite element analysis of electrical machines.* Norwell, MA: Kluwer (1995).

[15] Stępień S., Bernat J., *Modeling and optimal control of variable reluctance stepper motor.* COMPEL 30(2): 726-740 (2011).

[16] Vijayakumar K., Karthikeyan R., Paramasivam S. et al., *Switched Reluctance Motor Modeling, Design, Simulation, and Analysis: A Comprehensive Review.* IEEE Trans. Mag. 44(12): 4605-4617 (2008).

[17] Wang Y., Chau K., Chan C., Jiang J., *Transient analysis of a new outer-rotor permanent magnet brushless DC drive using circuit-field-torque coupled time-stepping finite element method.* IEEE Trans. Magn. 38(3): 1297-1300 (2002).

[18] Zhou P., Fu W., Lin D., Stanton S., Cendes Z., *Numerical modeling of magnetic devices*. IEEE Trans. Magn. 40(4): 1803-1809 (2004).